DNS AND LES WITH STOCHASTIC MODELLING OF SUBGRID ACCELERATION APPLIED TO SOLID PARTICLES IN A HIGH REYNOLDS NUMBER CHANNEL FLOW

Rémi Zamansky
LMFA CNRS UMR 5509
Ecole Centrale de Lyon
Ecully, F-69134, France
remi.zamansky@ec-lyon.fr

Ivana Vinkovic
LMFA CNRS UMR 5509
Université Lyon 1
Villeurbanne, F-69622, France
ivana.vinkovic@univ-lyon1.fr

Mikhael Gorokhovski
LMFA CNRS UMR 5509
Ecole Centrale de Lyon
Ecully, F-69134, France
mikhael.gorokhovski@ec-lyon.fr

ABSTRACT

Inertial particle acceleration statistics are analyzed using DNS in the case of a highly turbulent channel flow. Along with effects recognized in homogeneous isotropic turbulence, an additional effect is observed due to high and low speed vortical structures aligned with the channel wall. In response to those structures, the inertial particles experience strong longitudinal acceleration variations. DNS is also used in order to assess LES-SSAM (Subgrid Stochastic Acceleration Model), in which an approximation to the instantaneous non-filtered velocity field is given by simulation of both, filtered and residual, accelerations. Advantages of this approach in predicting particle dynamics in the channel flow at a high Reynolds number are shown.

INTRODUCTION

Understanding the Lagrangian behavior of inertial particles in turbulent channel flows has important implications for many environmental systems, from sediment transport to atmospheric dispersion of pollutants or solid deposition in marine flows. Previous experimental (Kaftori *et al.*, 1995) and numerical (Marchioli & Soldati, 2002) studies on particle-laden channel flows have examined particle deposition, trapping, segregation or the modification of particle velocity statistics due to the presence of coherent structures. It is recognized that inertial effects cause particle segregation and clustering (Kiger & Pan, 2002). In a high Reynolds number "free" turbulence (Bec *et al.*, 2006; Ayyalasomayajula *et al.*, 2008), these phenomena were coupled with particle acceleration statistics. In our paper, such statistics are of interest in the case of a high Reynolds number channel flow. This may help in understanding of complex interaction between particle dynamics and wall flow structures.

Lagrangian measurements (Ayyalasomayajula *et al.*, 2008; Qureshi *et al.*, 2008; Gerashchenko *et al.*, 2008) or computations (Marchioli & Soldati, 2002; Lavezzo *et al.*, 2010) provided insight into inertial particle accelerations and their statistics, including the acceleration probability density functions (PDF), in both homogeneous and inhomogeneous flows. These studies showed that, in the case of homogeneous isotropic turbulence, solid particles with low inertia exhibit highly non-Gaussian acceleration PDF with a high probability of intense acceleration events. These acceleration PDF tend to narrow and to gaussianize as particles inertia increases (Bec *et al.*, 2006). Bec *et al.* (2006) suggested that the trend of acceleration PDF to gaussianity, as well as a monotonic decrease of acceleration variance, are both a consequence of preferential concentration (dominant at small Stokes numbers) and filtering (for particles with larger Stokes numbers).

One could expect the same tendencies in the presence of the wall: preferential concentration and filtering may decrease the variance of particle acceleration. However, close to the wall, the flow is very different from homogeneous isotropic turbulence. There are typical streaks, aligned with the wall, characterized by alternating high and low longitudinal speed regions. Low inertia particles do not see this alternation of regions; once such particles get trapped in the structure, they travel with it. Highly inertial particles do not respond to this intermittency neither, due to the filtering effect. Only particles with intermediate inertia may respond to the spanwise alternation of high and low speed regions; this may cause an additional agitation of those particles. In this paper, particle acceleration statistics in the channel flow are explored, in comparison with the effects described by Bec *et al.* (2006) for the case of homogeneous isotropic turbulence.

For single phase flows, large-eddy simulation (LES) has become a suitable tool that produces acceptable results at much lower computational costs than direct numerical simulation (DNS). However, application of LES in turbulent channel flow becomes too expensive when the Reynolds number is high and the resolution of strong subgrid gradients is needed, specifically in the near-wall region, in the case of wall-bounded flows. An alternative to standard LES, referred to as LES-SSAM approach was proposed in Sabel´nikov *et al.* (2007, 2011). In this approach, the exact Navier-Stokes equation is replaced by a model equation in which the instantaneous total acceleration is viewed as a sum of two model accelerations. One represents the filtered acceleration closed by Smagorinsky model, another one emulates the residual (subgrid) acceleration. The later is done by two independent stochastic processes, for the norm of this acceleration and for its orientation. The new stochastic model for the subgrid acceleration was proposed in Zamansky *et al.* (2010), and was assessed in the case of turbulent channel flow in the framework of LES-SSAM approach. In this model, the norm of the subgrid acceleration is simulated stochastically, using statistical universalities in fragmentation under scaling symmetry (Gorokhovski & Saveliev, 2008). Its orientation is also simulated stochastically as a Brownian motion on a unit sphere, starting from random orientation on the wall plane, and then going toward stochastic isotropy away from the wall. Such a development of LES-SSAM approach (Zamansky *et al.*, 2010) will be applied to particle-laden channel flows. The accuracy of the method will be tested in regard of particle velocity and acceleration statistics. Results will be compared with DNS and classical LES. The tests will be run for different types of particles given by Stokes numbers from 1 to 125.

The article is organized as follows. In the next section, the numerical method is described. Then, we present some results obtained by DNS. In the last section, the LES-SSAM approach is compared to DNS and classical LES. Finally, conclusions are stated.

NUMERICAL METHOD

Flow

The flow considered is an incompressible turbulent channel flow. The computational domain consisting of two infinite parallel walls is illustrated in Figure 1. Periodic boundary conditions are imposed on the fluid velocity field in x (streamwise) and z (transverse) directions and no-slip boundary conditions are imposed at the walls.

Three different sets of numerical simulations for the fluid are treated here: direct numerical simulation of channel flow (DNS), standard large-eddy simulation (LES) and large-eddy simulation coupled with stochastic forcing of subgrid acceleration (LES-SSAM). For the case of LES the classical Smagorinsky model is used (Sagaut, 2002).

Details on the simulation characteristics are given in Table 1, where N_i and L_i are the number of grid points and the domain length in direction i. For all simulations, the Reynolds number based on the friction velocity u_τ, the channel half height h and the viscosity ν, is $Re_\tau \sim 587$. In the case of DNS, this corresponds to a Reynolds number based on the mean velocity U at the center of the channel of $Re \sim 12500$.

The incompressible Navier-Stokes equations in a turbulent channel flow are solved using a Galerkin spectral approximation (Fourier Chebyshev) and a variationnal projection method on a divergence free space (Buffat *et al.*, 2011). Steady state fluid statistics have been compared with other DNS by Zamansky *et al.* (2010).

Table 1. Simulation parameters.

Type	Re_τ	$N_x \times N_y \times N_z$	$L_x \times L_y \times L_z$
DNS	587	$384 \times 257 \times 384$	$3/2\pi h \times 2h \times 3/4\pi h$
LES	587	$64 \times 65 \times 64$	$3\pi h \times 2h \times \pi h$
LES-SSAM	587	$64 \times 65 \times 64$	$3\pi h \times 2h \times \pi h$

Particles Particles are injected into the flow at low concentrations in order to consider dilute systems. Particle-particle interactions are neglected as well as gravity or the influence of particles on the carrier fluid. Mirror conditions are applied for particle-wall bouncing. Furthermore, particles are considered to be point-wise, spherical, rigid and to obey the following Lagrangian dimensionless equation of motion :

$$St \frac{d\vec{v}_p}{dt} = \left(\vec{u} - \vec{v}_p\right) f(Re_p) \qquad (1)$$
$$\frac{d\vec{x}_p}{dt} = \vec{v}_p$$

Here, $\vec{v}_p$ and $\vec{x}_p$ are the dimensionless particle velocity and position. The solid particle - fluid interaction is modelled by a drag force with the correction term $f(Re_p) = 1 + 0.15Re_p^{0.687}$ suggested by Clift *et al.* (1978). Re_p is the local and instantaneous particle Reynolds number based on the local relative velocity, the particle diameter d_p and the fluid viscosity.

St is the Stokes number given by :

$$St = \frac{\tau_p}{\tau_f} \qquad (2)$$

with $\tau_p = \frac{\rho_p d_p^2}{18\rho\nu}$ and $\tau_f = \frac{\nu}{u_\tau^2}$, ρ_p and ρ being respectively the particle and fluid density. The Stokes number characterizes the response time of a particle to fluid solicitation.

Once the steady state for the fluid is obtained, 200000 particles are released at randomly chosen locations within the channel, then tracked at each time step. Five sets of particles are considered with $St = 1$, $St = 5$, $St = 15$, $St = 25$ and $St = 125$.

The initial velocities of the particles are set equal to the interpolated fluid velocities at each particle location. A high order three dimensional Hermite interpolation is used for computing the fluid velocity $\vec{u}(\vec{x}_p, t)$ at the particle position. The time-integration of the particle motion Equation (1) is performed using a second-order Adams-Bashforth method with the same time step as the DNS. Once the particles released, the simulations are run over several particle timescales τ_p. Particle statistics are sampled starting from $t^+ \sim 1000$,

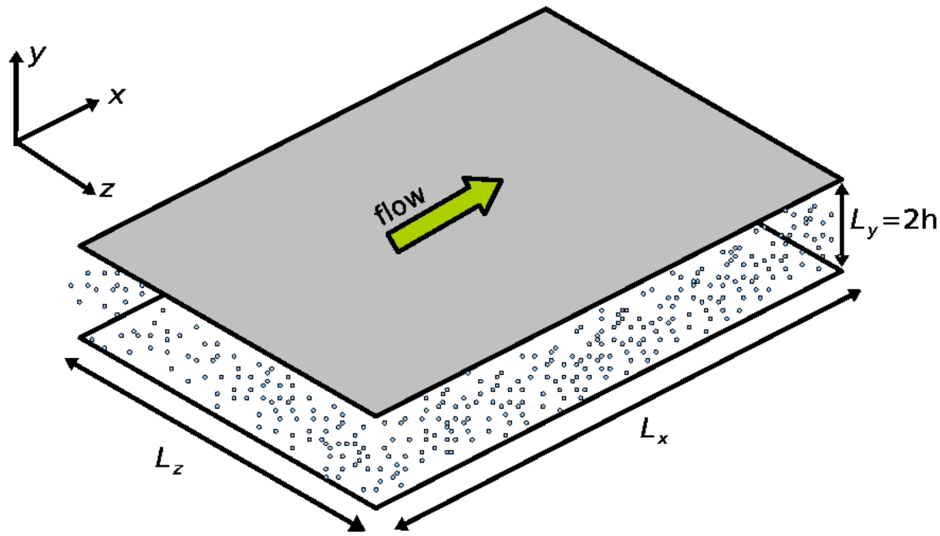

Figure 1. Channel flow. x, y, z represent the streamwise, the vertical and the transverse directions respectively.

counted from particle release. For all simulations, velocity statistics for the solid phase are at stationary state.

In this study, the acceleration is evaluated using the velocity time derivative along particle trajectories. Even though we use a three dimensional Hermite interpolation for computing the fluid velocity at particle position, as suggested by Choi *et al.* (2004) numerical errors are generated when a particle crosses a grid point. Therefore, as Mordant *et al.* (2004), the acceleration is estimated by a convolution of the Lagrangian velocity with the derivative of a Gaussian kernel. This ensures both time derivation and filtering. The filter width, of the order of τ_f, is such that there is agreement between fluid Lagrangian and Eulerian acceleration statistics.

In the case of DNS, for a lower Reynolds number, particle velocity statistics have been compared with the benchmark of Marchioli *et al.* (2008). For higher Reynolds numbers, velocity statistics have also been compared to the experiments of Lelouvetel *et al.* (2009). Details about these comparisons and other results based on particle velocity statistics may be found in Vinkovic *et al.* (2010).

DNS ACCELERATION STATISTICS

In this section we present some results obtained by DNS.

Acceleration variance Figure 2 shows the longitudinal acceleration variance of solid particles as a function of $y^+ = yu_\tau/\nu$. As the distance to the wall increases, the acceleration variance decreases. In addition to this, as particle inertia increases the acceleration variance departs from the fluid. This is in accordance with previous studies in homogeneous isotropic flows (Bec *et al.*, 2006; Ayyalasomayajula *et al.*, 2008; Calzavarini *et al.*, 2009) and results from the simultaneous effect of preferential concentration and filtering. For $St = 5$, the longitudinal acceleration variance presents the highest peak close to the wall. This peak is even higher than the fluid longitudinal acceleration variance. To get insight on this behavior, we analyze the acceleration statistics of the fluid seen by the solid particles.

Figure 3 illustrates the longitudinal acceleration variance of the fluid seen by the solid particles. The variance for the fluid seen by the solid particles is higher than the variance of the non-conditional fluid. This is especially the case close to the wall, at the position of the peak of longitudinal acceleration variance. The peak of fluid longitudinal acceleration at the solid particle position increases as the Stokes number increases. Whereas, the peak of solid particle acceleration first increases from $St = 1$ to $St = 5$ and then decreases as the Stokes number increases.

These observations suggest that in the case of wall bounded flow, the solid particles are entrained preferentially by regions with relatively high longitudinal acceleration variance. The contrary is observed in homogeneous isotropic turbulence (Bec *et al.*, 2006; Ayyalasomayajula *et al.*, 2008; Calzavarini *et al.*, 2009), where previous studies found that inertial particles tend to cluster in regions of the fluid experiencing relatively low fluid accelerations. In channel flow, the behavior of the solid particle longitudinal acceleration variance in the near wall region, suggests that because of particle inertia particles respond less and less to the increasingly varying fluid solicitations. This results in a net decrease of solid particle longitudinal acceleration variance.

Acceleration PDF In Figure 4 we compare the normalized PDF of longitudinal acceleration at $y^+ \sim 100$ for different Stokes numbers with the normalized PDFs obtained by using the fluid acceleration on the particle position. For reference, the normalized PDF for the non-conditional fluid acceleration is plotted as well. As expected, when the Stokes number increases, the tails of the normalized solid particle PDFs become narrower. For all Stokes numbers, the normalized PDFs of the fluid seen by the solid particles overlap almost perfectly with the normalized PDFs of the non-conditional fluid. The same conclusions can be drawn for other distances to the wall and for other components of the ac-

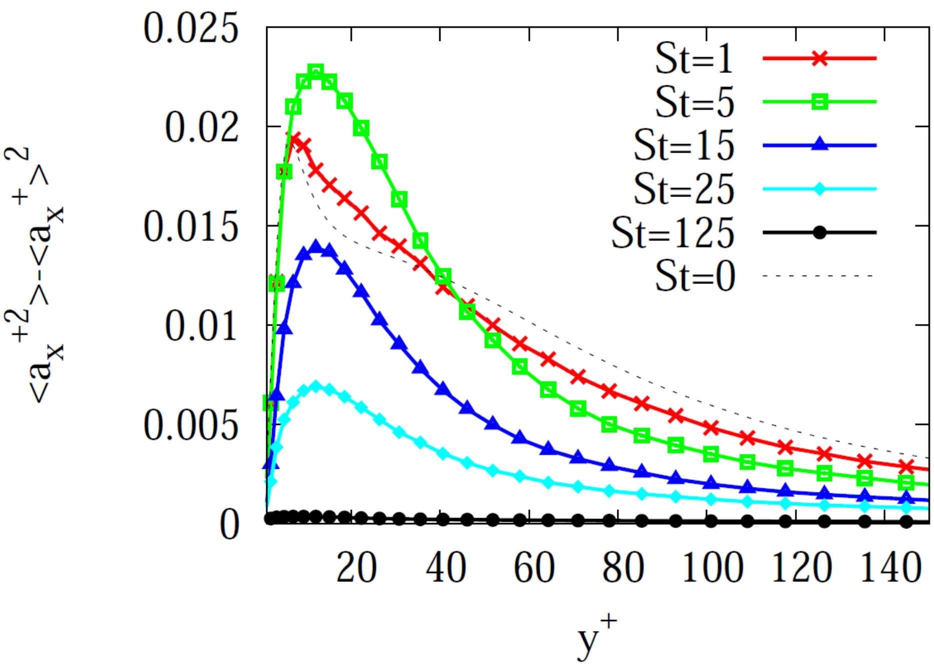

Figure 2. Longitudinal acceleration variance profile for solid particles with different Stokes numbers and for the fluid ($St = 0$).

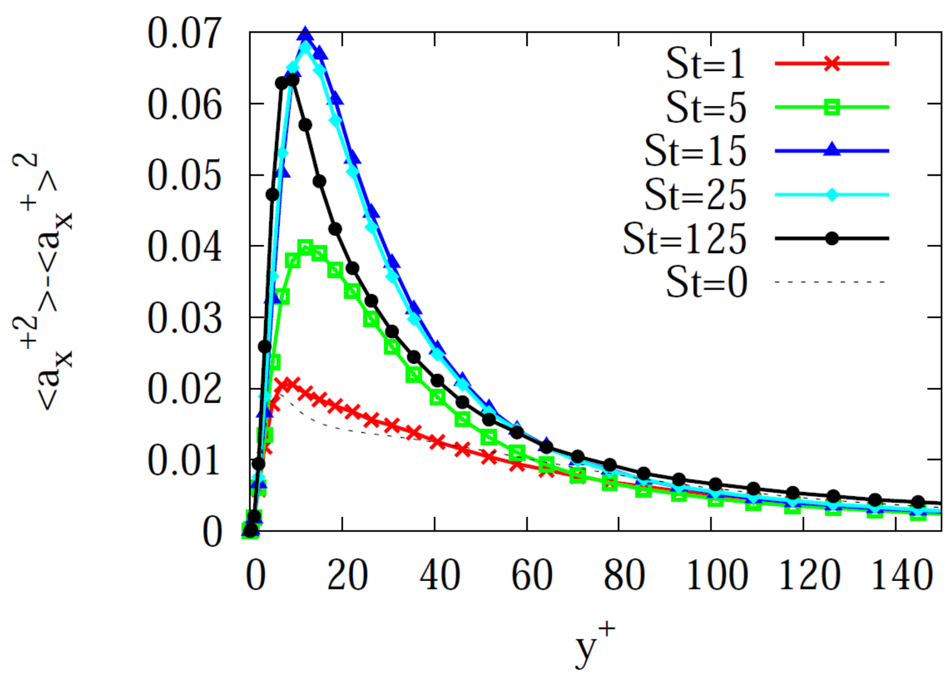

Figure 3. Longitudinal acceleration variance profile for the fluid seen by the solid particles with different Stokes numbers and for the fluid ($St = 0$).

celeration. For simplicity reasons, these plots are not shown here. The overlap suggests similarity of structure in terms of statistical distribution of fluid acceleration seen by the solid particles. The scaling factor is given by the acceleration RMS, which is different for each Stokes number.

These results show that in wall bounded flows, effects predicted by Bec *et al.* (2006) are present with a new aspect which is additional agitation of particles by alternation of high and low speed streaks. Wall bounded flows present spatial alternation of high and low speed vortical structures aligned with the channel wall. As in homogeneous isotropic turbulence, inertial particles are ejected from high vorticity regions toward high strain (high dissipation rate) regions. Inertial particles are swept by these regions and due to the random

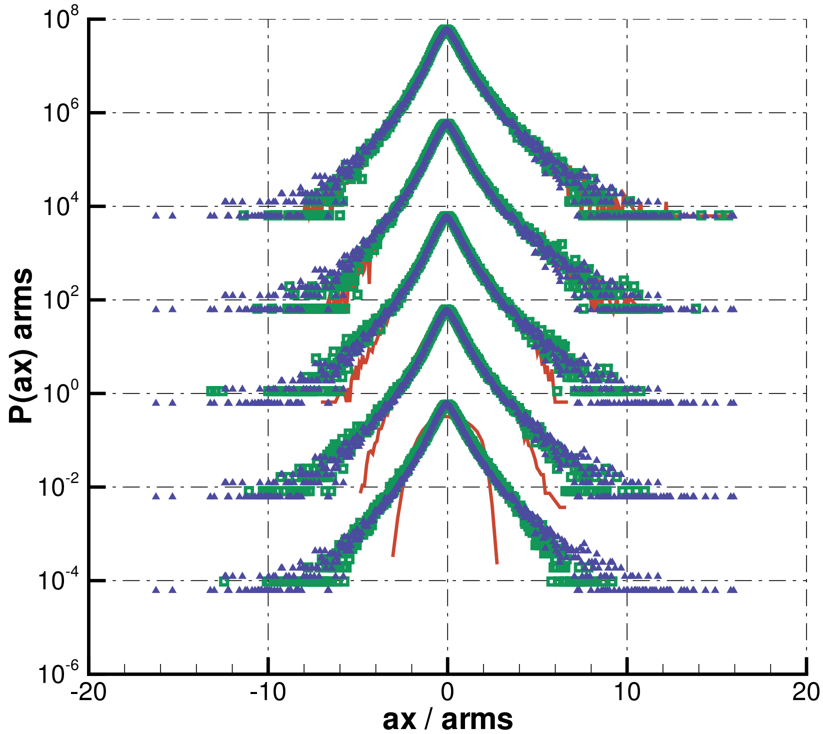

Figure 4. Longitudinal acceleration PDF at $y^+ = 100$, for (from top to bottom) $St = 1, 5, 15, 25, 125$. Solid particles (line), fluid particles (triangle), fluid seen by solid particles (square).

alternation of high and low speed streaks, experience strong longitudinal velocity fluctuations. Thereby, in these regions, inertial particles see fluid with high longitudinal acceleration variance. Slightly inertial particles (with a response time τ_p similar to the characteristic fluid timescale) may well respond to the fluid solicitations and therefore experience an increase of the longitudinal acceleration variance relatively to the fluid. Due to the filtering effect of inertia, very inertial particles ignore the wall turbulent structures and therefore present a more homogeneous concentration.

Here, the significance of wall structures on particle acceleration statistics has been shown. In the frame of LES, wall structures are under-resolved. Therefore, in the next section, classical LES is coupled with a stochastic model for subgrid acceleration in order to introduce flow intermittency at subgrid scales.

LES-SSAM APPLIED TO PARTICLES

Here we briefly describe the stochastic subgrid model for the acceleration used in the LES-SSAM approach. The LES-SSAM is then compared to classical LES and DNS in the case of particle laden turbulent channel flows.

LES-SSAM approach In order to take into account the non-resolved acceleration in standard LES, the approach proposed in Sabel´nikov *et al.* (2007) and Sabel´nikov *et al.* (2011) is used here. In this approach, the total instantaneous acceleration is given by two contributions : $a_i = \bar{a}_i + a'_i$. The first component is the filtered total acceleration where the overbar denotes the filtering operation. $\bar{a}_i$ is directly obtained by LES. The second component represents the total acceleration in the residual field, obtained by a stochastic model. When both parts are modeled, their sum gives an approximation to the non-filtered velocity field.

In the case of the channel flow, a model for the subgrid acceleration was proposed in Zamansky *et al.* (2010). In comparison with standard LES, it was showed that the LES-SSAM approach gives better prediction of velocity spectra on small spatial scales and better statistics of fluid acceleration. In the following section, we apply this model to the case a of particle laden channel flow.

Results and comparisons Figures 5 and 6 show the solid particle mean and RMS velocity profiles obtained from the LES-SSAM model and compared to the DNS and LES results. The LES-SSAM model gives a better estimation of the mean solid particle velocity than classical LES (Figure 5). In addition to this, there is also an improvement of the prediction of the vertical (Figure 6) velocity RMS profile.

Figure 7 illustrates the transverse component RMS of the solid particle acceleration. As described in the previous sec-

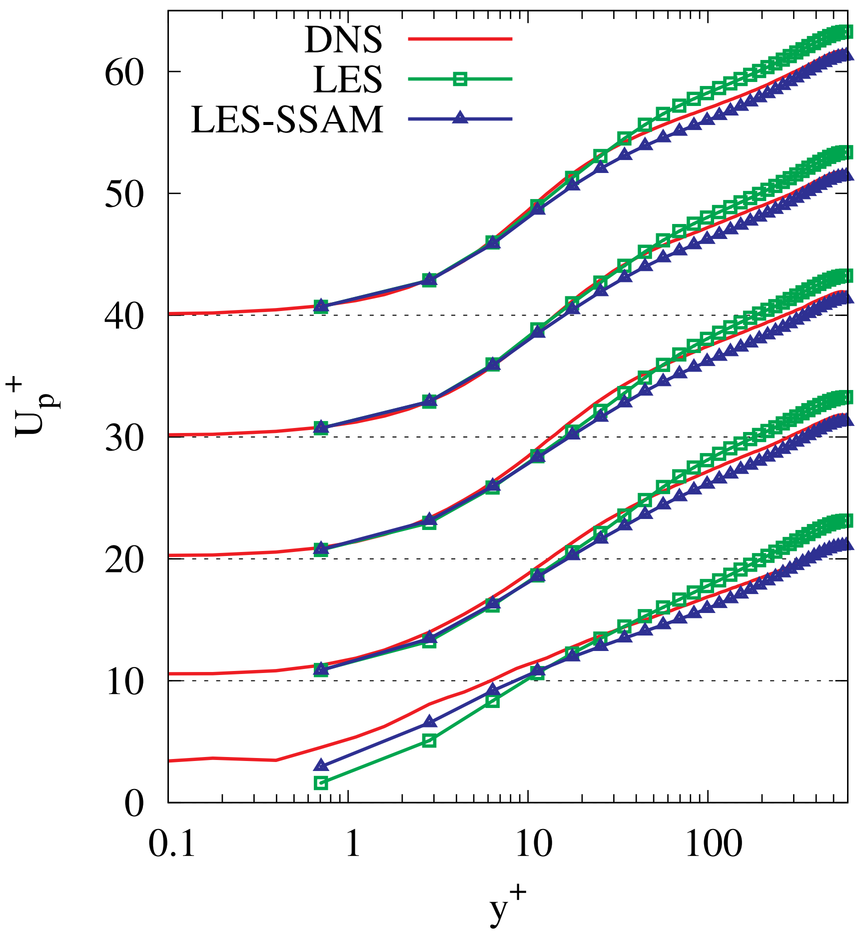

Figure 5. Mean longitudinal velocity profile of solid particles for (from top to bottom) $St = 1, 5, 15, 25, 125$. DNS (line), LES (squares), LES-SSAM (triangles).

tion, when the Stokes number increases the RMS of solid particle acceleration decreases. This evolution is well reproduced by LES-SSAM, while standard LES predicts much lower values of the acceleration RMS. For other components of the acceleration we observe either the same improvement either no difference with classical LES.

CONCLUSIONS

In this study, numerical simulations of particle laden turbulent channel flow are performed for five different Stokes numbers and a high Reynolds number. Acceleration statistics obtained by DNS show that in wall bounded flows, effects predicted in homogeneous isotropic turbulence (Bec *et al.*, 2006) are completed by a new aspect which is additional agitation of particles by alternation of high and low speed streaks. As in homogeneous isotropic flows, inertial particles are ejected from high vorticity regions toward high strain (high dissipation rate) regions. Due to the proximity of high and low speed streaks, particles experience strong longitudinal acceleration variations. Depending on their inertia particles may well respond to those fluid solicitations (experiencing an increase of the longitudinal acceleration variance) or ignore the wall turbulent structures (presenting in that case a more homogeneous concentration).

In order to take intermittency effects into account at subgrid scales, a model for the subgrid acceleration is introduced according to Zamansky *et al.* (2010). The capability of LES-SSAM for particle-laden turbulent channel flow is assessed by comparing the results with DNS and classical LES. The LES-SSAM model gives a better estimation of the solid particle velocity and acceleration statistics.

Along with fundamental interest, the LES-SSAM approach has a practical relevance, when significant physics take place on subgrid scales. In such conditions, simulations at a high Reynolds number warrant advanced subgrid models that account for intermittency effects on small spatial scales. In future studies, the LES-SSAM approach will be applied to the simulation of vaporization, and combustion in two-phase flows.

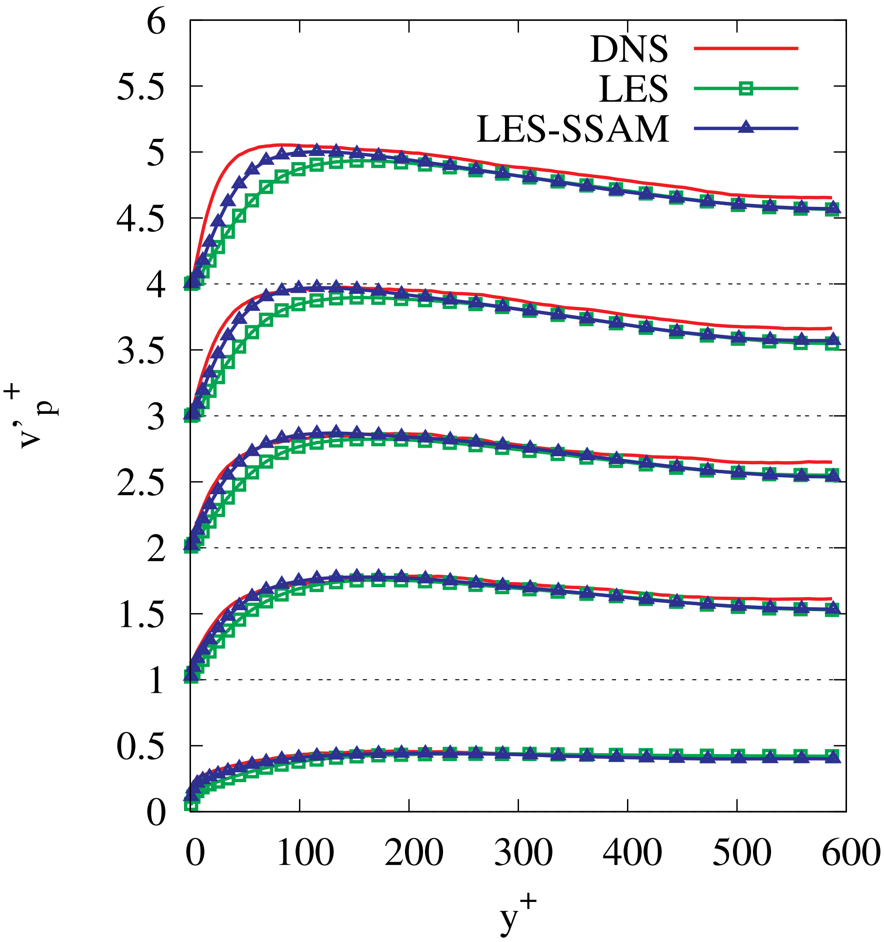

Figure 6. Vertical velocity RMS profile of solid particles for (from top to bottom) $St = 1, 5, 15, 25, 125$. DNS (line), LES (squares), LES-SSAM (triangles).

ACKNOWLEDGMENTS

M. Buffat is acknowledged for the development of the computational code. The authors express their gratitude to F. Laadhari who kindly provided his initial fields for the DNS. This work was granted access to the HPC resources of CINES under the allocation 2009-c200902560 made by GENCI (Grand Equipement National de Calcul Intensif). Numerical simulations were also performed on the P2CHPD parallel cluster. The authors are therefore grateful to C. Pera for the administration of the computational tool.

REFERENCES

Ayyalasomayajula, S., Warhaft, Z. & Collins, L.R. 2008 Modeling inertial particle acceleration statistics in isotropic turbulence. *Phys. Fluids* **20**, 095104.

Bec, J., Biferale, L., Boffetta, G., Celani, A., Cencini, M., Lanotte, A., Musacchio, S. & Toschi, F. 2006 Acceleration statistics of heavy particles in turbulence. *J. Fluid Mech.* **550**, 349–358.

Buffat, M., Penven, L. Le & Cadiou, A. 2011 An efficient spectral method based on an orthogonal decomposition of the velocity for transition analysis in wall bounded flow. *Comput. Fluids* **42**, 62–72.

Calzavarini, E., Volk, R., Bourgoin, M., Lévêque, E., Pinton, J.-F. & Toschi, F. 2009 Acceleration statistics of finite-sized particles in turbulent flow: the role of Faxén forces. *J. Fluid Mech.* **630**, 179–189.

Choi, J.-I., Yeo, K. & Lee, C. 2004 Lagrangian statistics in turbulent channel flow. *Phys. Fluids* **16:3**, 779–793.

Clift, R., Grace, J.R. & Weber, M.E. 1978 *Bubble, Drops and Particles*. Academic Press.

Gerashchenko, S., Sharp, N.S., Neuscamman, S. & Warhaft, Z. 2008 Lagrangian measurements of inertial particle accelerations in a turbulent boundary layer. *J. Fluid Mech.* **617**, 255–281.

Gorokhovski, M. & Saveliev, V. 2008 Statistical universalities in fragmentation under scaling symmetry with a constant frequency of fragmentation. *J. Phys. D: Appl. Phys.* **41**, 085405.

Kaftori, D., Hestroni, G. & Banerjee, S. 1995 Particle behaviour in the turbulent boundary layer. I. Motion, deposition and entrainment. *Phys. Fluids* **7:5**, 1095–1106.

Kiger, K.T. & Pan, C. 2002 Suspension and turbulence modifi-

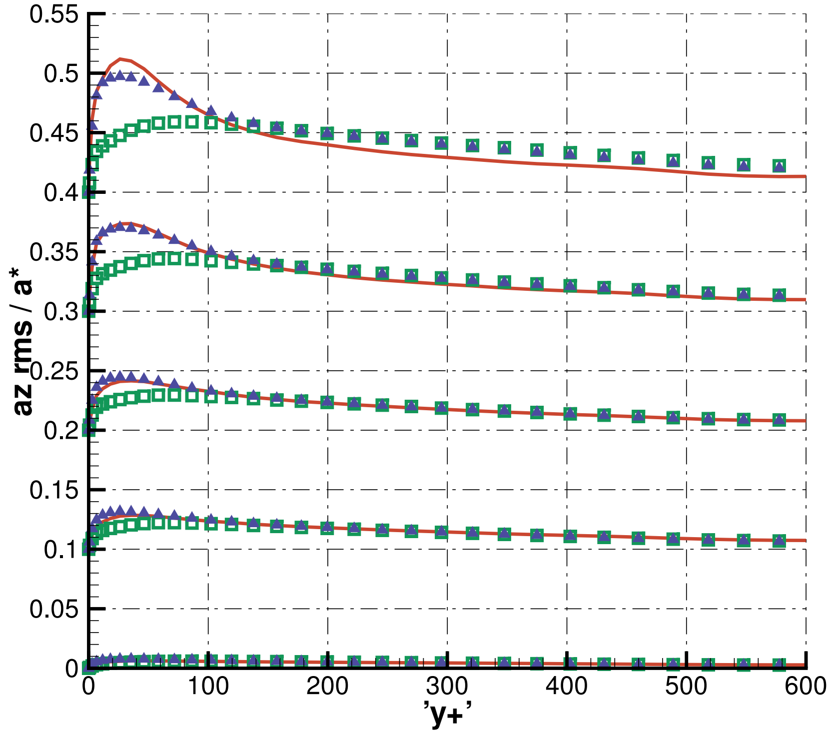

Figure 7. Transverse acceleration RMS profile of solid particles for (from top to bottom) $St = 1, 5, 15, 25, 125$. DNS (line), LES (squares), LES-SSAM (triangles).

cation effects of solid particulates on a horizontal turbulent channel flow. *J. of Turbulence* **3**, 1–21.

Lavezzo, V., Soldati, A., Gerashchenko, S., Warhaft, Z. & Collins, L.R. 2010 On the role of gravity and shear on inertial particle accelerations in near-wall turbulence. *J. Fluid Mech.* **658**, 229–246.

Lelouvetel, J., Bigillon, F., Doppler, D., Vinkovic, I. & Champagne, J.-Y. 2009 Experimental investigation of ejections and sweeps involved in particle suspension. *Water Resour. Res* **45**.

Marchioli, C. & Soldati, A. 2002 Mechanisms for particle transfer and segregation in a turbulent boundary layer. *J. Fluid Mech.* **468**, 283–315.

Marchioli, C., Soldati, A., Kuerten, J.G.M., Arcen, B., Tanière, A., Goldensoph, G., Squires, K.D., Cargnelutti, M.F. & Portela, L.M. 2008 Statistics of particle dispersion in direct numerical simulations of wall-bounded turbulence: Results of an international collaborative benchmark test. *Int. J. Multiphase Flow* **34**, 879–893.

Mordant, N., Crawford, A. M. & Bodenschatz, E. 2004 Experimental lagrangian acceleration probability density function measurement. *Physica D* **193**, 245–251.

Qureshi, N.M., Arrieta, U., Baudet, C., Cartellier, A., Gagne, Y. & Bourgoin, M. 2008 Acceleration statistics of inertial particles in turbulent flow. *Eur. Phys. J. B* **66**, 531–536.

Sabel´nikov, V., Chtab, A. & Gorokhovski, M. 2007 The coupled LES-sub-grid stochastic acceleration model (LES-SSAM) of a high Reynolds number flow. In *Advances in Turbulence XI* (ed. Springer), , vol. 117, pp. 209–211. 11th EUROMECH European Turbulence Conference.

Sabel´nikov, V., Chtab-Desportes, A. & Gorokhovski, M. 2011 New sub-grid stochastic acceleration model in LES of high-Reynolds-number flows. *Eur. Phys. J. B* **80**, 177–187.

Sagaut, P. 2002 *Large Eddy Simulation for Incompressible Flows: An introduction*. Springer Verlag, second edition.

Vinkovic, I., Doppler, D., Lelouvetel, J. & Buffat, M. 2010 Direct numerical simulation of particle interaction with ejections in turbulent channel flows. *Int. J. Multiphase Flow* p. doi:10.1016/j.ijmultiphaseflow.2010.09.008.

Zamansky, R., Vinkovic, I. & Gorokhovski, M. 2010 LES approach coupled with stochastic forcing of subgrid acceleration in a high-Reynolds-number channel flow. *J. Turbulence* pp. 1–18.